# Optical Analogue of Electronic Bloch Oscillations

Riccardo Sapienza,* Paola Costantino, and Diederik Wiersma
*European Laboratory for Nonlinear Spectroscopy and INFM,† 50019 Sesto Fiorentino (Florence), Italy*

Mher Ghulinyan,‡ Claudio J. Oton,§ and Lorenzo Pavesi
*Department of Physics, University of Trento and INFM,‖ I-38050 Povo (Trento), Italy*
(Received 11 August 2003; published 23 December 2003)

We report on the observation of Bloch oscillations in light transport through periodic dielectric systems. By introducing a linear refractive index gradient along the propagation direction the optical equivalent of a Wannier-Stark ladder was obtained. Bloch oscillations were observed as time-resolved oscillations in transmission, in direct analogy to electronic Bloch oscillations in conducting crystals where the Wannier-Stark ladder is obtained via an external electric field. The observed oscillatory behavior is in excellent agreement with transfer matrix calculations.

DOI: 10.1103/PhysRevLett.91.263902 PACS numbers: 42.70.Qs, 42.25.Dd, 42.25.Hz, 71.20.–b

A quantum particle in a periodic potential (a crystal) is described by Bloch waves, which are delocalized in space and exhibit an energy spectrum characterized by conduction bands and energy gaps. If such a particle is accelerated by a constant external field, its velocity will increase until it reaches the Brillouin band edge where the energy band dispersion leads to a net reduction of the particle velocity. The particle velocity reaches zero at the band edge and then changes sign. This phenomenon is known as electronic Bloch oscillations [1,2]. Bloch oscillations were predicted by Bloch and Zener already in 1928 [1], which led to several controversies that continued for over 60 years [3]. One of the issues was the counterintuitive result that an external stationary field could lead to an oscillating current. The first confirmation of the Bloch-Zener model came as the observation of a Wannier-Stark ladder when an external stationary field was applied to a crystal [4]. The Wannier-Stark ladder is the frequency domain counterpart of time-resolved Bloch oscillations and consists of the formation of equidistant energy levels in the electron band structure. Electronic Bloch oscillations in regular crystals are difficult to observe because electrons lose their coherence on time scales much faster than the expected Bloch oscillation period. The advent of semiconductor superlattices [5] partially solved this problem since the oscillation period in these systems is much faster [6]. Time-resolved Bloch oscillations were then indeed observed on superlattice systems [7,8].

There exist fascinating analogies between electron transport and transport of optical waves in dielectric structures [9]. Ordered (periodic) dielectric systems are called photonic crystals and can exhibit a photonic band gap in analogy with the electronic band gap in semiconductors [10]. Quasiperiodic dielectric systems like Fibonacci quasicrystals can also be realized [11] and exhibit interesting time-resolved transport properties [12]. In disordered systems the optical counterpart of weak localization [13], Anderson localization [14], short and long range correlations [15], and universal conductance fluctuations [16] have all been observed. These are various examples of wave phenomena where interference effects play a crucial role both in the optical and the electronic cases. Often these processes are easier to study with light because the coherence time of an optical wave packet is usually much longer than that of an electronic wave packet. This naturally raises the question whether it is possible to mimic the effect of an electric field in photonic systems and observe the optical counterpart of electronic Bloch oscillations.

The optical equivalent of a Wannier-Stark ladder has been discussed theoretically [17], and different photonic systems have been proposed to observe Bloch oscillations of light waves [18,19]. In pioneering experiments on two-dimensional dielectric systems, spatial Bloch oscillations have been observed [20]. These experiments intrinsically rely on a two-dimensional structure, however, since the light wave follows an oscillatory path in space due to lateral confinement [19]. Optical superlattices have been proposed as a potentially ideal system to observe Bloch oscillations for light waves, using a refractive index gradient *parallel* to the light propagation direction as the optical equivalent of an external force (the static electric field in the electron case) [21].

In this Letter we report on the experimental observation of time-resolved optical Bloch oscillations. This observation was performed in time-resolved transmission experiments on optical superlattices. A linear gradient in the optical thickness was used to provide longitudinal confinement of the optical wave packet by tilting the photonic band structure, in direct analogy to the electron case. We confirm experimentally that the oscillation period depends linearly on the optical thickness gradient. We calculate the expected behavior of the system via a standard transfer matrix model and find very good agreement between theory and experimental observations.

An optical superlattice can be obtained in one dimension by stacking two types $A$ and $B$ of dielectric multilayers. In particular, we used the following sequence:

  

*BABABABAB* $(AA)_1$ *BABABABAB* $(AA)_2$ ... $(AA)_{10}$ *BABABABAB*. This structure is a series of $m$ coupled microcavities $(AA)_m$ where the *BABABABAB* substructure functions as a Bragg reflector. The refractive indices of layers $A$ and $B$ were taken, $n_A = 1.4$ and $n_B = 2.1$, to obtain good optical contrast between the layers. The physical thickness of each layer was chosen such that the optical thickness $\delta \equiv n \times d$, with $n$ the refractive index and $d$ the physical layer thickness, was equal to $\lambda/4$. This way each cavity has the minimum required thickness to be resonant at $\lambda$. Taking thicknesses that are multiples of $d$ would provide similar results but require growing thicker samples. The optical coupling between the microcavities is tuned by changing the reflectivity of the Bragg reflectors and causes the formation of extended photonic states, in analogy to the electronic coupling of separate quantum wells in a superlattice. When identical microcavities are coupled, degenerate mode repulsion arises. Each degenerate optical resonance splits up and a photonic miniband forms. Because of the periodicity of the structure the photonic minibands are separated by photonic band gaps in which propagation is prohibited.

To obtain Bloch oscillations, the one-dimensional translational symmetry of the system should be broken. This is done by introducing a gradient in the optical thickness of the layers, given by $\Delta\delta = (\delta_{z_m} - \delta_{z_1})/\delta_{z_1}$. This gradient is the optical counterpart of the external electric field used in electronic superlattices. The gradient changes slightly the resonance of each microcavity while preserving the mode coupling, which results in a spatial tilting of the minibands and the photonic band gaps. In this way, the extended photonic states are turned into a discrete sequence of energy levels with level spacing $\Delta E_B$, which is the optical equivalent of the Wannier-Stark ladder.

Transfer matrix calculations can be used conveniently to calculate the scattering states map of the light distribution inside our system. In Fig. 1, the light intensity distribution is compared for the two cases $\Delta\delta = 0$ and 14%. The linear gradient in the optical thickness induces, to first order, a linear miniband tilting. The resonance of the first microcavity is given by $E(z_1) = hc/2\delta_{z_1}$ with $c$ the vacuum velocity of light. The variation of the resonance energy from layer 1 to layer $m$ is $\Delta E(z_1, z_m) = E(z_1) - E(z_m)$ and can be written in terms of the gradient as

$$\frac{\Delta E(z_1, z_m)}{E(z_1)} = \frac{1}{1 + \Delta\delta} - 1. \qquad (1)$$

This describes a linear tilt and compression of the band. For a narrow miniband, $E(z_1)$ can be considered constant within the band and the Wannier-Stark states are equidistant. In Fig. 1(b) one can clearly see how the miniband (between the white dashed lines) and surrounding photonic band gaps (dark regions) are tilted. The Wannier-Stark states are visible as bright horizontal lines that extend between the two tilted photonic band gaps. Such a system is expected to exhibit optical Bloch oscillations of period $T_B = h/\Delta E_B$, where $h$ is the Planck constant.

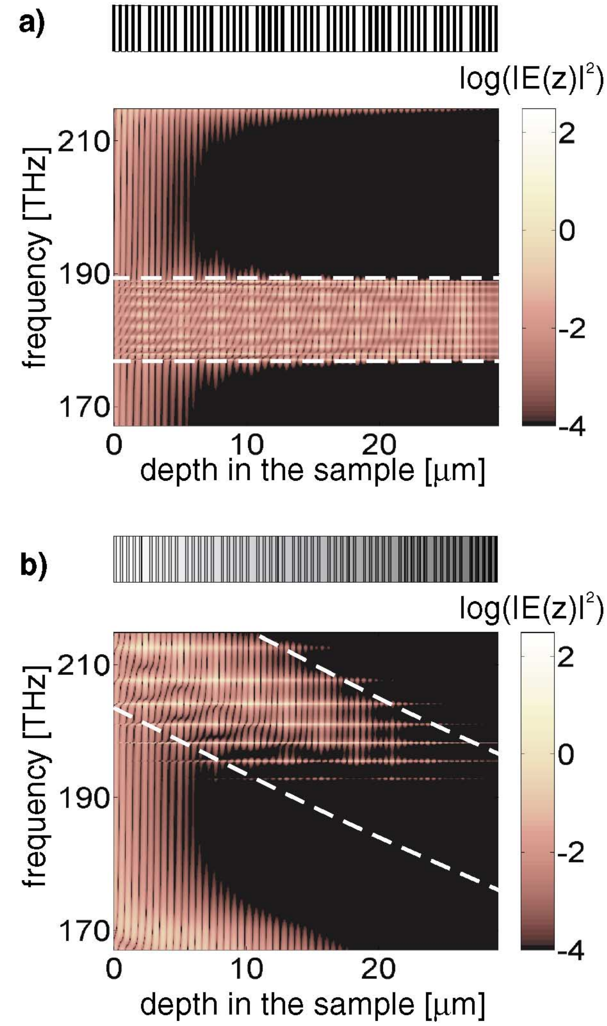


FIG. 1 (color online). Scattering state calculation of the distribution of the energy spectrum inside an optical superlattice composed of ten coupled microcavities. The parameters used in the calculations correspond to samples used in the actual experiment. (a) Flat band situation, $\Delta\delta = 0$. (b) Tilted band situation, $\Delta\delta = 14\%$. The dashed lines indicate the theoretical tilting of the miniband as obtained from Eq. (1). Above each panel the coupled microcavity structure is schematically shown; the gray scale refers to the refractive index variation along the depth in the sample (darker $\equiv$ larger $n$).

The samples were realized using controlled etching of silicon [22,23]. The refractive index of porous silicon depends on the porosity, which in turn depends on the current density used in the electrochemical etch. This allows the production of dielectric multilayers by modulating the current and hence the local porosity during the etching process. The electrochemical etch parameters determine the thickness and refractive index of each layer. We used (100)-oriented $p^+$-type Si wafers (resistivity 0.01 $\Omega$ cm). The electrolyte was prepared mixing 30 vol % aqueous HF (48 wt.%) with ethanol. A current density of 50 $mA/cm^2$ was used to obtain the low refractive index $A$ layers ($n_A = 1.4$, etch duration 5.9 s) and 7 mA/cm$^2$ for the high refractive index $B$ layers ($n_B = 2.1$, etch duration 21.5 s), where $\lambda = 1.55$ $\mu$m. By alternating these two currents we created samples formed by ten coupled microcavities as described before. The total sample consisted of 110 layers.

The samples were made freestanding by detaching them from the silicon substrate with a high current pulse at the end of the etch (400 mA/cm$^2$, 1 s). The exchange of the electrolyte was improved via etch stops after each layer and the use of a magnetic stirrer. Moreover, the natural refractive index drift was compensated by changing the etching times of the layers. The duration of the etch stops controls the refractive index gradient and hence the variation $\Delta\delta$ in the optical thickness of each layer. We produced samples with different gradients in the range from $\Delta\delta = 2\%$ to 14%. In Fig. 2 we report the transmission spectrum for a sample with gradient $\Delta\delta = 10\%$. One can clearly see the occurrence of a Wannier-Stark ladder as a series of narrow transmission peaks.

In order to perform time-resolved transmission experiments, an optical gating technique has been applied. This involves mixing a reference beam together with the transmitted signal in a 0.3 mm thick nonlinear (beta barium borate) crystal to produce a sum frequency signal. The probe beam is obtained from an optical parametric oscillator pumped by a Ti:sapphire laser at center wavelength 810 nm (pulse duration 130 fs, average power 2.0 W, repetition rate 82 MHz) yielding short pulses tunable from 1300 to 1600 nm (average power 100 mW). The reference pulse at 810 nm is obtained from the residual Ti:sapphire beam (450 mW average power). The sum frequency signal is detected by a photodiode, and a standard lock-in technique is used to suppress noise. A delay line in the reference beam allows one to tune the time delay between signal and reference. In the top panel of Fig. 3 the system response, as obtained without sample, is plotted. The temporal resolution is 250 fs. The apparatus is designed such that the transmission spectrum of the sample can also be monitored during the time-resolved measurement by sampling a small fraction of the transmitted light.

Figure 3 shows a series of time-resolved transmission measurements for various values of the gradient $\Delta\delta$. Our transfer matrix calculations predict that above $\Delta\delta \approx 7\%$ a Wannier-Stark ladder is formed in our samples. From the time-resolved data we can observe that indeed oscillations occur in transmission. More than eight periodic oscillations are observed in the transmitted intensity, with a period $T_B$ that decreases as $\Delta\delta$ increases. In addition, as the gradient increases the transmitted intensity decreases, which can be understood from the increased tilt of the band gap (see also Fig. 1). The oscillations are damped with a characteristic time $\tau_B$.

The main parameter ruling the dynamics of Bloch oscillations is the oscillation period $T_B$. In Fig. 4 we compare the measured $T_B$ with the one extracted from our transfer matrix model for various values of the gradient. As expected, the experimentally observed values of $T_B$ decrease while increasing $\Delta\delta$ because the miniband tilting gets steeper. The period depends only on the relative energy tilting from the front to the end of the sample and not on the sample thickness. Below $\Delta\delta \approx 7\%$ the increase of $T_B$ saturates. Here the optical thickness gradient is not enough to fully tilt the miniband within the sample thickness, and the remaining oscillations are simply due to internal reflection at the sample boundaries. In this regime the residual variation in $T_B$ of a few percent is due to a decrease in the optical coupling between the microcavities. The experimental data are in very good agreement with the calculated theoretical dependence of $T_B$ on optical thickness gradient (solid line).

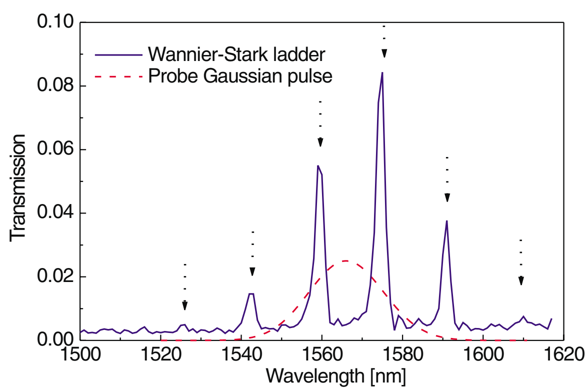


FIG. 2 (color online). Transmission spectrum of a sample with gradient $\Delta\delta = 10\%$. The optical equivalent of the Wannier-Stark ladder is seen as a series of equidistant transmission peaks (2 nm full width at half maximum and 15 nm spaced). The arrows refer to the expected spectral positions of the transmission peaks obtained by transfer matrix calculations. The dashed line is the wavelength profile of the incident Gaussian laser pulse used to perform the time-resolved measurements.

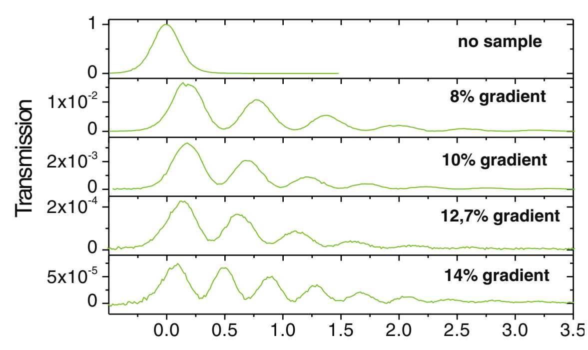


FIG. 3 (color online). Temporal response of the system for various values of the gradient $\Delta\delta$. The observed oscillations are the optical counterpart of time-resolved Bloch oscillations. The period of the oscillations decreases while increasing $\Delta\delta$, and the transmission decreases. The top panel reports the undisturbed probe pulse without sample.

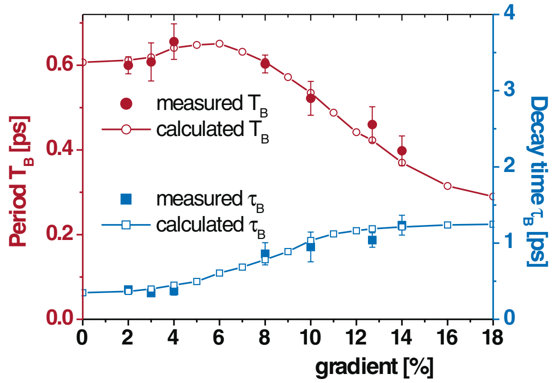


FIG. 4 (color online). Experimentally observed oscillation period $T_B$ and decay time $\tau_B$ as a function of the gradient $\Delta\delta$. The error bars are the standard deviations obtained from various measurements on several positions on the sample and represent therefore the effect of lateral sample inhomogeneities. The solid line is the predicted behavior from transfer matrix calculations.

Another interesting observation in Fig. 4 is that the decay time $\tau_B$ by which the oscillations are damped increases when $\Delta\delta$ increases. This is a direct consequence of the increased confinement of the optical modes in the Wannier-Stark ladder. As the gradient gets steeper, the reflection at the band edge becomes more efficient and the transmission losses decrease accordingly. At large gradient values, $\tau_B$ saturates to about 1.2 ps. This saturation is caused by scattering and residual absorption losses in the porous silicon sample. Hence the total decay time $\tau_B$ can be written as $\tau_B = (\tau_{pBO}^{-1} + \tau_{\rm ext}^{-1})^{-1}$, where $\tau_{pBO}$ is the intrinsic decay time of the Bloch oscillation as due to the release of energy from the system and $\tau_{\rm ext}$ is the extinction time due to absorption and scattering losses. The solid line in Fig. 4 is obtained by taking $\tau_{\rm ext} \sim 1.3$ ps which corresponds to an extinction coefficient (absorption + scattering) of $\alpha_{\rm ext} \sim 100\ {\rm cm}^{-1}$, in agreement with previously determined loss values [23].

In conclusion, we have observed the optical counterpart of electronic Bloch oscillations in optical superlattices of porous silicon. A linear variation in the optical constants of the system along the propagation direction allows the formation of a Wannier-Stark ladder and to observe optical Bloch oscillations resolved in time. Both the oscillation period and the damping time versus the strength of the Wannier-Stark ladder are consistent with predictions from transfer matrix calculations.

We thank Luca Dal Negro, Fausto Rossi, Claudio Andreani, Maurizio Artoni, Marcello Colocci, and Roberto Righini for discussions. This work was financially supported by INFM projects Rands and Photonic and by MIUR through FIRB Project No. RBNE012N3X.

*Electronic address: sapienza@lens.unifi.it
†Electronic address: www.complexphotonics.com
‡Electronic address: mghool@science.unitn.it
§Present address: Department of Fundamental Physics, University of La Laguna, La Laguna 38204 Tenerife, Spain.
||Electronic address: www.science.unitn.it/~semicon/

[1] F. Bloch, Z. Phys. **52**, 555 (1928); C. Zener, Proc. R. Soc. London A **145**, 523 (1934).
[2] H. M. James, Phys. Rev. **76**, 1611 (1949); G. H. Wannier, Phys. Rev. **100**, 1227 (1955).
[3] See, e.g., C. F. Hart and D. Emin, Phys. Rev. B **37**, 6100 (1988); J. Zak, Phys. Rev. B **43**, 4519 (1991).
[4] A. G. Chynoweth, G. H. Wannier, R. A. Logan, and D. E. Thomas, Phys. Rev. Lett. **5**, 57 (1960).
[5] L. Esaki and R. Tsu, IBM J. Res. Dev. **14**, 61 (1970).
[6] E. E. Mendez, F. Agullo-Rueda, and J. M. Hong, Phys. Rev. Lett. **60**, 2426 (1988); J. Bleuse, G. Bastard, and P. Voisin, Phys. Rev. Lett. **60**, 220 (1988).
[7] See, e.g., J. Feldmann *et al.*, Phys. Rev. B **46**, 7252 (1992); K. Leo *et al.*, Solid State Commun. **84**, 943 (1992).
[8] T. Dekorsky, P. Leisching, K. Köhler, and H. Kurz, Phys. Rev. B **50**, 8106 (1994); V.G. Lyssenko *et al.*, Adv. Solid State Phys. **38**, 257 (1998).
[9] See, e.g., Ping Sheng, *Introduction to Wave Scattering, Localization, and Mesoscopic Phenomena* (Academic Press, New York, 1995).
[10] See, e.g., *Photonic Bandgap Materials*, edited by C. M. Soukoulis (Kluwer, Dordrecht, 1996); J. D. Joannopoulos, R. D. Meade, and J. N. Winn, *Photonic Crystals* (Princeton University Press, Princeton, NJ, 1995).
[11] W. Gellermann, M. Kohmoto, B. Sutherland, and P. C. Taylor, Phys. Rev. Lett. **72**, 633 (1994).
[12] L. Dal Negro *et al.*, Phys. Rev. Lett. **90**, 055501 (2003).
[13] Y. Kuga and A. Ishimaru, J. Opt. Soc. Am. A **8**, 831 (1984); M. P. van Albada and A. Lagendijk, Phys. Rev. Lett. **55**, 2692 (1985); P. E. Wolf and G. Maret, Phys. Rev. Lett. **55**, 2696 (1985).
[14] R. Dalichaouch *et al.*, Nature (London) **354**, 53 (1991); A. Z. Genack and N. Garcia, Phys. Rev. Lett. **66**, 2064 (1991); D. S. Wiersma *et al.*, Nature (London) **390**, 671 (1997).
[15] N. Garcia and A. Z. Genack, Phys. Rev. Lett. **63**, 1678 (1989); M. P. van Albada, J. F. de Boer, and A. Lagendijk, Phys. Rev. Lett. **64**, 2787 (1990).
[16] F. Scheffold and G. Maret, Phys. Rev. Lett. **81**, 5800 (1998).
[17] G. Monsivais, M. del Castillo-Mussot, and F. Claro, Phys. Rev. Lett. **64**, 1433 (1990); C. M. de Sterke *et al.*, Phys. Rev. E **57**, 2365 (1998).
[18] G. Lenz, I. Talanina, and C. M. de Sterke, Phys. Rev. Lett. **83**, 963 (1999); A. Kavokin *et al.*, Phys. Rev. B **61**, 4413 (2000).
[19] P. B. Wilkinson, Phys. Rev. E **65**, 056616 (2002).
[20] T. Pertsch *et al.*, Phys. Rev. Lett. **83**, 4752 (1999); R. Morandotti *et al.*, Phys. Rev. Lett. **83**, 4756 (1999).
[21] G. Malpuech *et al.*, Phys. Rev. B **63**, 035108 (2001).
[22] O. Bisi, S. Ossicini, and L. Pavesi, Surf. Sci. Rep. **38**, 1 (2000).
[23] M. Ghulinyan *et al.*, J. Appl. Phys. **93**, 9724 (2003).